A luminescence spectroscopy study of SrI2:Nd3+ single crystals

Article *in* Journal of Luminescence · November 2013
DOI: 10.1016/j.jlumin.2013.04.007

6 authors, including:

Igor N. Ogorodnikov
Ural Federal University
206 PUBLICATIONS **966** CITATIONS
SEE PROFILE

V.A. Pustovarov
Ural Federal University
308 PUBLICATIONS **1,192** CITATIONS
SEE PROFILE

Alina Goloshumova
Sobolev Institute of Geology and Mineralogy
15 PUBLICATIONS **66** CITATIONS
SEE PROFILE

L. I. Isaenko
Sobolev Institute of Geology and Mineralogy
298 PUBLICATIONS **2,856** CITATIONS
SEE PROFILE

Journal of Luminescence. V.143. November 2013. Pages 101–107. DOI: 10.1016/j.jlumin.2013.04.007

A luminescence spectroscopy study of $SrI_2:Nd^{3+}$ single crystals

I.N. Ogorodnikov[a,*], V.A. Pustovarov[a], A.A. Goloshumova[b], L.I. Isaenko[b], A.P. Yelisseyev[b], V.M. Pashkov[b]

[a] *Experimental Physics Department, Ural Federal University, 19, Mira Street, 620002 Ekaterinburg, Russia*
[b] *Institute of Geology and Mineralogy of Siberian Branch of RAS, 43, Russkaya Street, 630058 Novosibirsk, Russia*

Abstract

The paper presents the results of a study on the luminescence of $SrI_2:Nd^{3+}$ single crystals grown by the vertical Bridgman method. The photoluminescence (PL) spectra of SrI_2:Nd crystals show characteristic lines corresponding to transitions in trivalent Nd^{3+} ions, the most intense line at ca.1070 nm is due to the radiative $^4F_{3/2} \rightarrow {}^4I_{11/2}$ transitions. Efficient PL excitation in a crystal transparency band occurs due to optical $4f - 4f$ transitions from the ground $^4I_{9/2}$ state, or the charge transfer transitions $I^- \rightarrow Nd^{3+}$. The paper discussed two new PL emission bands at 2.8 and 3.8 eV, associated with the lattice defects formed in SrI_2 crystal at introducing Nd^{3+} impurity ions; two intense narrow PL excitation bands at 5.52 and 5.31 eV, originating from free and defect-bound excitons, respectively; an efficient channel of exciton energy transfer between the host lattice and defects. We calculated the $H(k)$ functions of distribution of the elementary relaxations over the reaction rate constants and explained on this basis the nonexponential PL decay kinetics in $SrI_2:Nd^{3+}$ crystal.

Keywords:
Time-resolved luminescence spectroscopy, strontium iodide SrI_2, trivalent Nd^{3+} ion, exciton energy transfer, PL decay kinetics

1. Introduction

Scintillation crystals are now an important part of many applications, including the detection of gamma radiation with high energy resolution to identify isotopes. Among the commercially available inorganic scintillators, $LaBr_3$:Ce is leading in the energy resolution of ca.2.6 % at 662 keV [1–3]. Alkaline earth metal iodides represent another outstanding family of fluorescent crystals. In this series, $SrI_2:Eu^{2+}$ emits light in the Eu^{2+} photoluminescence (PL) band (λ= 435 nm, τ= 1.2 μs [4, 5]), shows the highest light output (over 120 photons/keV [6]), excellent energy resolution (2.6 % at 662 keV [7]), and a high proportionality of light yield [8]. Many research works were devoted to optimize a composition and improve the energy transfer processes in strontium iodide crystals. For instance, Gahane et al. [9] studied the luminescence of Eu^{2+} ions in the matrices of $KI{\cdot}2\,BaI_2$ and $KI{\cdot}2\,SrI_2$ and CaI_2. The SrI_2(Ce/Na) system was studied in [6, 8]. Other trivalent ions have not been tested in the SrI_2 system, while $LaBr_3$ crystals doped with Nd^{3+} impurity ions have recently been developed and successfully applied in a fast $LaBr_3:Nd^{3+}$ scintillator with the PL lifetime of τ= 15 ns, light yield ca.20 photons/keV and the energy resolution of 7.5 % [10, 11]. We are not aware of such publications on SrI_2:Nd, although $SrI_2:Nd^{3+}$ crystals can be considered as a model system to better understand the SrI_2 host lattice doped with heterovalent impurity ions of trivalent rare earth elements. There are important reasons to choose Nd^{3+} impurity ions to study the problem. Indeed, as some of the rare earth elements, neodymium ion can be in the divalent or trivalent charge state. However, unlike the other rare earth elements, neodymium ion forms steady compounds, such as iodide, which is essential for doping by heterovalent impurity ions. The compensation of the excess charge in this case can be done by uncontrolled intrinsic lattice defects or intentionally introduced alkali metal ions. Note also that in addition to the above applications, the neodymium ions in various matrices are widely used in a variety of optical applications, such as the working material for lasers operating in the near infrared spectral range.

*Corresponding author. Tel.: +7 (343) 3754711; fax: +7 (343) 3743884.
Email address: i.n.ogorodnikov@gmail.com (I.N. Ogorodnikov)

Postprint published online *April, 2013*

The main goal of this work is a study of luminescence properties of SrI_2:Nd single crystals using a time-resolved vacuum ultraviolet (VUV) spectroscopy technique upon selective excitation by synchrotron radiation in a broad energy range. The main attention was paid to the processes in the SrI_2:Nd host lattice and the energy transfer from the matrix to the Nd^{3+} impurity ions. The present work does not include the detailed spectroscopic study of the processes occurring inside the Nd^{3+} ions. The data on the spectroscopy of Nd^{3+} ions have been published in numerous publications, such as [12–14]. In our study, these data were used to identify the Nd^{3+} ions in the luminescence spectra of SrI_2:Nd^{3+}.

2. Experimental details

All the examined crystals, SrI_2 and SrI_2:Nd doped with the 2.5 mol. % Nd^{3+} ions, were grown at the Institute of Geology and Mineralogy of Siberian Branch of Russian Academy of Sciences (Novosibirsk) utilizing the vertical Bridgman method. The starting materials were SrI_2 and NdI_3 (melting points are 515 and 775°C, respectively). All details of the obtaining of SrI_2 were described in [15, 16]. The mixture of strontium iodide and 2.5 % neodymium iodide was placed to a silica ampoule, which then was evacuated, sealed and placed in a two-zone furnace. The resulting composition was heated to 780°C. The crystal growth began with spontaneous nucleation. To ensure a flat crystallization front the optimal pulling speed and vertical temperature gradient in the growth zone were 1–4 mm/h and 30–35°C/cm, respectively. The size of grown crystals was $\oslash 15\times 40\,mm^3$. Samples were cut from a clean part of crystal boule, which was 25 mm in length. The sizes of the investigated crystals were $6\times 5\times 1.5\,mm^3$; the largest surfaces studied were cleaved and parallel. The concentration of the Nd^{3+} impurity ions was chosen to make its luminescence comparable in intensity with the other PL emission bands found previously in SrI_2 crystals [16]. Data on the real structure of the grown crystals of strontium iodide were presented in a previous paper [16]. X-ray diffraction study showed that crystal structure parameters of SrI_2:Nd crystals have no significant deviations from that of pure SrI_2 presented in [17].

Because of hygroscopic nature of SrI_2 crystals, any contact with the atmospheric air leads to degradation of the sample surface that becomes cloudy due to the formation of crystalline hydrates. In this regard, each SrI_2:Nd sample after preparation was kept in an evacuated and sealed ampoule. In all our experiments the samples were removed from the ampoules, cleaved in an atmosphere of a dry hot air and immediately mounted in the sample holder attached to a He-flow cryostat with a fast vacuum pumping. Before starting the VUV experiments the samples were kept in a cryostat for 12 h at T= 90°C in a vacuum not worse than 10^{-6} Torr. After that, we performed spectroscopic measurements in a vacuum better than 7×10^{-10} Torr.

The present study was carried out by the means of the low-temperature luminescence VUV spectroscopy with the time-resolution. The PL emission spectra in the energy range of E_m from 1.2 eV to 5.0 eV and the PL excitation (PLE) spectra in the energy range of E_{ex} from 3.7 eV to 20 eV (spectral resolution 0.32 nm) were recorded at the temperatures of 8 and 293 K at the SUPERLUMI experimental station of HASYLAB (DESY, Germany) [18] upon excitation with synchrotron radiation (SR). At the storage ring DORIS the full width at half maximum (FWHM) of synchrotron radiation pulses was 130 ps with the repetition period of 96 ns. Such pulses excitation enables the recording of spectra within a time-window correlated with the arrival of SR pulses. In the present experiments we recorded time-resolved spectra within two independent time-windows (TWs) set for detection of luminescence signal within 1.4–14.0 ns (TW1) and 52.5–72.5 ns (TW2) relative to the beginning of the SR pulse. Time-integrated (TI) spectra were recorded within the full time range available between two sequential excitation pulses, viz. 96 ns. The primary 2 m-vacuum monochromator, equipped with Al-grating was used for selective PL excitation with synchrotron radiation. The PL excitation spectra were corrected to an equal number of photons incident on the sample using sodium salicylate with the energy-independent quantum yield over the studied spectral range. The 0.3 m ARC Spectra Pro-300i monochromator equipped with an R6358P (Hamamatsu) photomultiplier were used as a registration system. The PL emission spectra were not corrected to the spectral sensitivity of the recording system.

The PL characteristics upon excitation in the visible and UV spectral region were measured at 293 K. The 1 kW xenon discharge lamp and the primary MDR-2 grating monochromator were used as an excitation source. The secondary SDL-1 spectrophotometer and the cooled FEU-83 photomultiplier tube were used as a registration system to record photoluminescence in the visible to near infra red spectral region. The PLE spectra were normalized to an equal number of photons incident on the sample, whereas the PL emission spectra are shown without correction.

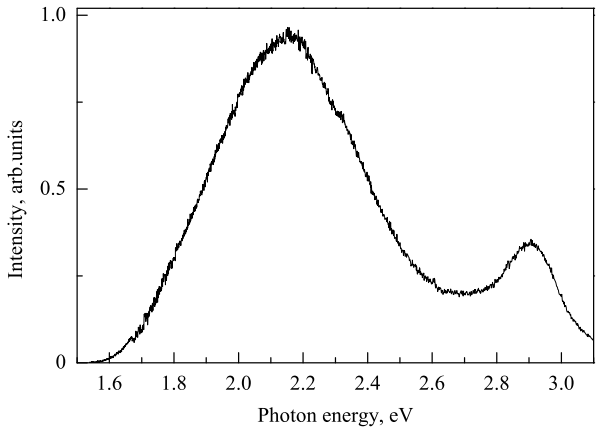

Figure 1: PL emission spectrum recorded for undoped SrI_2 crystal at T= 293 K upon excitation at λ_{ex}= 350 nm (3.54 eV).

3. Experimental results and Discussion

3.1. Undoped SrI_2 *crystals*

Undoped crystals of SrI_2 are transparent in a wide spectral range, the crystal transparency band has a short-wavelength edge at ca.300 nm. Photoexcitation of undoped SrI_2 crystals at λ_{ex}= 350 nm (3.54 eV) and T= 293 K results in PL emission in the yellow spectral region, Fig. 1. The PL emission spectrum comprises of two broad bands at 2.2 and 2.9 eV (FWHM= 0.55 and 0.22 eV), respectively. The 2.2 eV band can be caused by crystal hydrates, that arose in the interaction of the SrI_2 surface with the water molecules as it was shown previously for SrI_2:Eu [16]. Spectroscopic parameters of the low-intensity 2.9 eV band are the same as for the $5d \rightarrow 4f$ luminescence of Eu^{2+} in SrI_2 crystals. On the basis of spectroscopic data we suggest that the undoped SrI_2 crystals could contain traces of unintentionally introduced Eu^{2+} ions.

3.2. Luminescence spectroscopy of Nd^{3+} *ions in* SrI_2:Nd *crystals*

Deep red PL emission spectra. Luminescent properties of SrI_2:Nd crystals differ substantially from those of undoped SrI_2 crystals. The main difference lies in the manifestation of intense radiative transitions in Nd^{3+} impurity ions. Inset in Fig. 2 shows the energy diagram of trivalent Nd^{3+} ion composed on the basis of the numerical data [12, 13]. The spectroscopic properties of neodymium impurity ions in the present study were investigated in the visible and near infrared spectral region. Fig. 2 shows a fragment of the steady-state luminescence spectrum of SrI_2:Nd crystal recorded at T= 293 K in the spectral range of 925–1150 nm upon excitation at λ_{ex}= 330 nm. The dominant PL emission band at 1060–1080 nm and less intensive band at 975–990 nm correspond to the intra-configuration transitions from the lowest excited state $^4F_{3/2}$ onto the levels of $^4I_{11/2}$ and $^4I_{9/2}$, respectively. These transitions are chosen as the most intense and informative because $^4F_{3/2}$ manifold contains only two Stark levels, and $^4I_{9/2}$ manifold contains five Stark levels and is the ground state of $4f^3$ shell in Nd^{3+} ion. Energy diagram (Fig. 2) suggests the possibility of other radiative transitions, but they have much lower PL intensities in comparison with the dominant PL emission band.

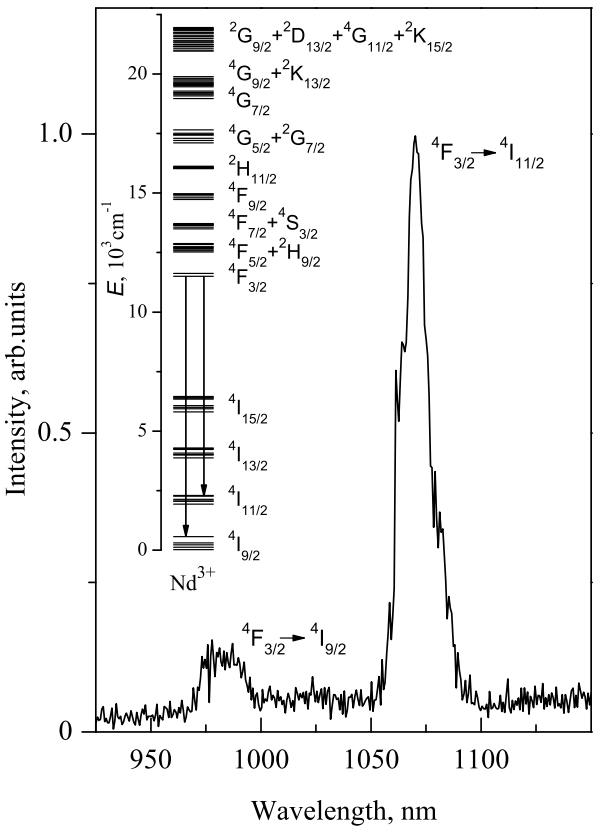

Figure 2: PL emission spectrum recorded for SrI_2:Nd crystal at T= 293 K upon excitation at λ_{ex}= 330 nm (3.76 eV). Inset shows the Nd^{3+} energy diagram composed using numerical data [12, 13].

PLE spectra. PLE spectrum of the dominant emission band at 1070 nm was recorded in the energy range of 300–1050 nm, which corresponds to optical transitions from the $^4I_{9/2}$ ground state onto the excited states of $^4F_{3/2}$, $^2H_{9/2}$ + $^4F_{5/2}$, $^4S_{3/2}$ + $^4F_{7/2}$, $^4G_{7/2}$, $^4G_{9/2}$, and $^4G_{11/2}$ in Nd^{3+} ion, Fig. 3. At wavelengths shorter than 390 nm PLE spectrum comprises a dominant complex

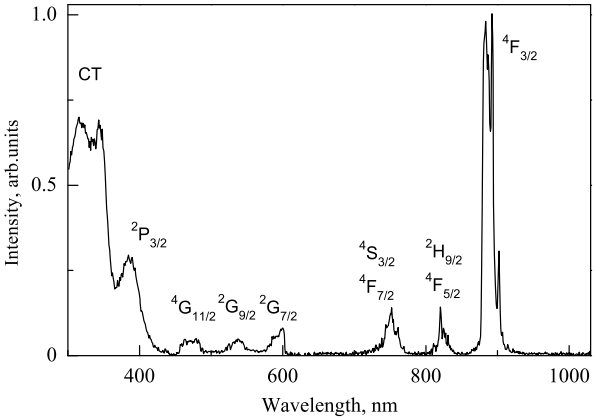

Figure 3: PLE spectrum recorded for SrI_2:Nd crystal at T= 293 K monitoring emission at 1070 nm. Labels indicate the lines of the identified transitions from the ground $^4I_{9/2}$ state to labeled excited levels in Nd^{3+} ion.

band, which is caused by charge-transfer transitions $I^- \rightarrow Nd^{3+}$. The energy position of the charge-transfer absorption band in SrI_2:Nd crystal (Fig. 3) is comparable to the published data on the charge-transfer bands of crystals $CaGa_2S_4$:Nd [19] and YI_3:Nd [20]. The experimental data on the luminescence of SrI_2:Nd crystals (Fig. 2 and 3) clearly indicate the presence of Nd^{3+} impurity ions in the SrI_2 host lattice. At the same time, the concentration of trivalent Nd^{3+} ions seems fairly low, because they do not provide a significant contribution to the optical absorption or transmission spectra of SrI_2:Nd crystals. Let us discuss the possible prerequisites for introduction of Nd^{3+} impurity ions into SrI_2 host lattice.

From a crystallographic point of view, SrI_2 belongs to the orthorhombic crystal system (space group *Pbca*), its unit cell contains eight formula units (24 atoms) and characterized by lattice parameters a= 1.522, b= 0.822, c= 0.790 nm, and it has a specific weight ρ= 4.549 g cm^{-3} [17, 21, 22]. The SrI_2 unit cell contains eight equivalent Sr^{2+} ions and two non-equivalent sets of eight I^- ions. Such a lattice is not a cubic structure, and can not be represented as a slightly distorted cubic structure. Such a lattice can not be described in terms of cubic symmetry, or presented as a slightly distorted cubic structure. The observed splitting of ^4F PLE band (Fig. 3) also suggests non-cubic local symmetry of Nd^{3+} sites in SrI_2 crystals. The ionic radii of Nd^{3+} and Sr^{2+} are 112.3 and 132 pm, respectively [23], which favors the heterovalent substitution of Sr^{2+} host ion by Nd^{3+} impurity ion. The compensation of the excess charge of the impurity ion in this case can be done by either alkali metal ions or structural lattice defects. In this case,

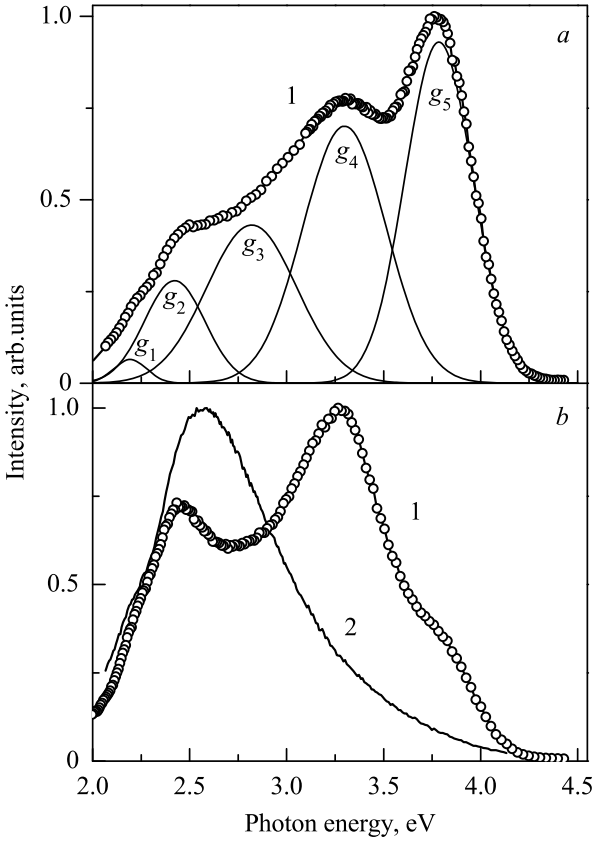

Figure 4: The time-integrated (TI) PL emission spectra recorded in the energy range of 2.0–4.5 eV for SrI_2:Nd crystal at 8 (1) and 293 K (2) upon excitation at E_{ex}= 5.29 (*a*) and 5.39 eV (*b*). The open circles and curve (2) show the experimental data. Symbols $g_1 \ldots g_5$ indicate the principal isolated elementary Gaussian bands.

the compensation of the excess charge of the impurity ion can be done by either monovalent alkali metal ions or structural lattice defects. However at this stage we should not exclude the possibility that Nd^{3+} impurity ions can occupy interstitial voids in the SrI_2 host lattice.

It should be noted that we do not expect the introduction of divalent Nd^{2+} ions into the SrI_2 host lattice. Indeed, despite the isovalent nature of Nd^{2+} impurity ion, its ionic radius (143 pm) exceeds the radius of Sr^{2+} host ion that requires considerable lattice distortion in the vicinity of the impurity ion. In addition, we have not detected the expected spectroscopic manifestations of the radiative $4f^1\,5d - 4f^2$ transitions in Nd^{2+} ions. Such transitions have been previously observed in the form of a weak broad band at 560 nm in SrB_4O_7:Nd [24] and CaF_2:Nd [25].

3.3. *Luminescence spectroscopy of lattice defects in* SrI_2:Nd *crystals*

Visible and near-UV PL emission spectra. In the visible and near-ultraviolet (UV) spectral region, the PL emission spectrum of SrI_2:Nd crystal contains broad bands that can not be associated with the radiative transitions in neodymium ions. Fig. 4 shows the time-integrated (TI) PL emission spectra of SrI_2:Nd crystal, measured in the energy range of 2.0–4.5 eV. Profile of PL spectrum depends on the excitation energy E_{ex}. At E_{ex}= 5.29 eV, the low-temperature PL emission spectrum consists of two intense broad bands at 3.3 and 3.75 eV, and two well-defined shoulders at 2.2 and 2.5 eV. At E_{ex}= 5.39 eV the PL emission spectrum changed in profile. In this case, the low-temperature PL emission spectrum consists of broad bands at 2.45 and 3.25 eV, and shoulders at 2.2 and 3.75 eV. At room temperature, the PL emission spectrum consists of a broad complex band at 2.6 eV, which shows a gradual decrease in intensity of high-energy slope from 2.6 to 4.5 eV. Decomposition of PL emission spectrum has identified five principal elementary Gaussian bands labeled as $g_1 \dots g_5$, Fig. 4. A set of these bands describe all the observed PL emission spectra shown in Fig. 4. The difference between these spectra is only in the relative intensities of the elementary bands. Comparison of the band parameters (Tab. 1) indicates that the low temperature PL emission spectrum is dominated by two bands of g_4 and g_5, which together are responsible for more than half of the light sum. However, the ratio of their contributions depends on the excitation energy. At E_{ex}= 5.29 eV, g_5-band has the highest intensity in PL emission spectrum and determines ca.35 % of the light sum. At E_{ex}= 5.39 eV, g_4-band dominates and determines ca.42 % of the light sum, whereas the contribution of g_5-band is reduced by more than three times. At room temperature, the PL emission spectrum is determined by the contribution of the other two bands of g_2 and g_3, which together provide more than 70 % of the light sum, Tab. 1.

Table 1: Parameters of the $g_1 \dots g_5$ elementary bands being responsible for the PL emission spectra recorded for SrI_2:Nd crystals, energy position (E_m), full width at half maximum (FWHM), band intensity normalized to 100 conventional units at the observed maximum of the PL spectrum (I_m), percentage contribution of the elementary band into the total light sum of the PL emission spectrum (S), exciting photons energy (E_{ex}), and temperature (T).

Parameter	PL emission band				
	g_1	g_2	g_3	g_4	g_5
E_m, eV	2.19	2.42	2.82	3.30	3.78
FWHM, eV	0.20	0.37	0.55	0.51	0.41
E_{ex}= 5.29 eV, T= 8 K					
I_m, arb.units	6.5	28.0	43.1	70.1	93.0
S, %	1.2	9.4	21.6	32.6	35.1
E_{ex}= 5.39 eV, T= 8 K					
I_m, arb.units	12.3	57.3	51.9	90.8	29.3
S, %	2.2	19.2	25.9	42.1	10.5
E_{ex}= 5.39 eV, T= 293 K					
I_m, arb.units	12.5	43.9	44.1	23.0	6.0
S, %	4.4	28.4	42.5	20.6	4.2

PLE spectra. Fig. 5 shows PLE spectra recorded at 8 and 293 K monitoring time-integrated emission of different PL bands at E_m. The common feature of these spectra is that in all cases the most efficient PL excitation occurs in a rather narrow energy range from about 5 to 6 eV. At other excitation energies, the luminescence intensity is quite low. PLE spectrum recorded monitoring emission at E_m= 3.87 eV is the most structured,

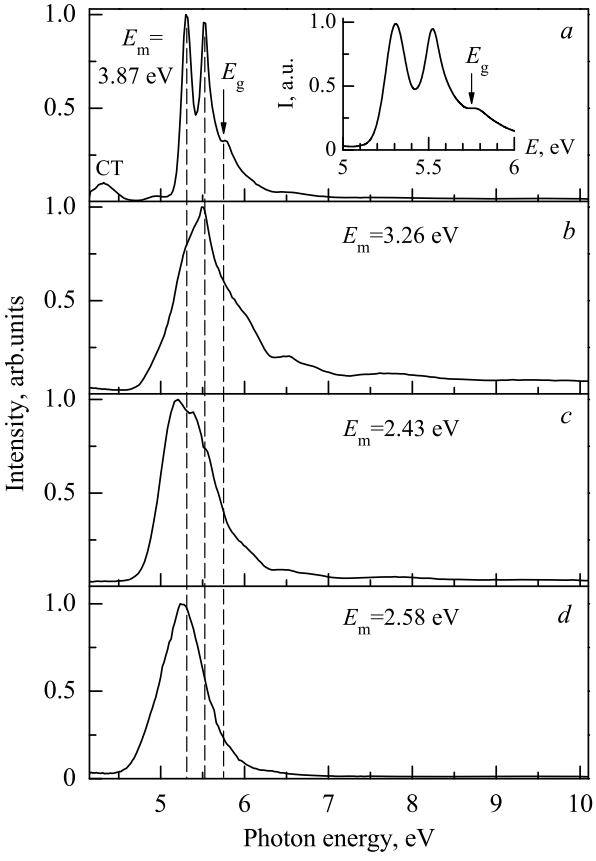

Figure 5: PLE spectra recorded for SrI_2:Nd crystal at 8 (*a–c*) and 293 K (*d*) monitoring time-integrated emission at E_m. The vertical arrow indicates the position of E_g according to the data [16]. Inset shows an enlarged fragment of PLE spectrum in the energy range from 5 to 6 eV.

it consists of two partially overlapped intense narrow bands with sharp peaks at 5.31 and 5.52 eV (FWHM= ca.0.15 eV). The low-energy slope of the PLE spectrum is characterized by the cut-off energy of ca.5.15 eV. The high-energy slope exhibits a pronounced local minimum at 5.75 eV.

PLE spectra recorded monitoring emission at the other bands (Fig. 5, *b–d*) are less structured, and their low-energy tails extend down to the low-energy region up to 4.5 eV. The position of the maximum intensity in these spectra varies slightly for different experimental conditions. At T= 8 K peaks in PLE spectra are located at 5.19 eV (E_m= 2.43 eV) and 5.50 eV (E_m= 3.26 eV). At room temperature, PLE maximum is located at 5.26 eV (E_m= 2.58 eV).

Isolated low-intensity bands at 4.30 and 4.95 eV, which are observed only in the PLE spectrum for E_m= 3.87 eV, are due to charge-transfer transitions $I^- \rightarrow Nd^{3+}$, Fig. 5, *a*. In the 6–10 eV energy range, PLE efficiency is not high, but it is different for different PL bands: the higher intensity is observed in PLE spectrum recorded monitoring emission at E_m= 3.26 eV, Fig. 5, *b*.

Our results (Figs. 4, 5, Tab. 1) in combination with the earlier data on SrI_2:Eu luminescence [16] allow us to make reasonable assumptions about the nature of $g_1 \ldots g_5$ bands. According to spectroscopic parameters, two of the lower-energy bands g_1 and g_2 are comparable to the PL emission bands from crystal hydrates, which result from the interaction of the SrI_2 surface with water molecules. Low-temperature band g_4 is comparable to the 3.4 eV luminescence band [16], which is due to radiative annihilation of self-trapped excitons in the SrI_2 crystal. The remaining two elementary bands g_3 and g_5 can not be compared with the data on SrI_2 (Fig. 1) and previous results on SrI_2:Eu [16]. These PL emission bands should be attributed to the presence of Nd^{3+} impurity ions in the SrI_2 host lattice.

In our opinion, the narrow PLE peak at 5.31 eV (Fig. 5, *a*) is due to a creation of excitons in the vicinity of the defect complexes consisting of Nd^{3+} impurity ion and associated defect, which is needed to compensate for the excess charge of the trivalent impurity. Spectroscopic parameters of this peak are close to that for the exciton peak at 5.52 eV in PLE spectrum (Fig. 5, *a*). Defect-bound exciton can relax by transferring energy to both the Nd^{3+} impurity ion and associated charge-compensating defect. The presence of the 5.52 eV peak in PLE spectrum indicates the existence of an effective channel of exciton energy transfer from the matrix to the defect complexes. From Fig. 5, *a* it follows that PLE efficiency of the Nd^{3+} luminescence is much higher for excitonic channel than that for the charge-transfer transitions. PL emission band g_3 is efficiently excited in the entire investigated temperature range of 8–293 K, and it should be attributed to the luminescence of the charge-compensating defect. At the same time, the spectroscopic properties of the low-temperature PL emission band g_5 is similar to those of g_4-band, which is due to radiative annihilation of self-trapped excitons in SrI_2. This allows us to discuss the possible connection of PL emission band g_5 with radiative annihilation of self-trapped excitons in the vicinity of the discussed defect complexes in the SrI_2:Nd host lattice.

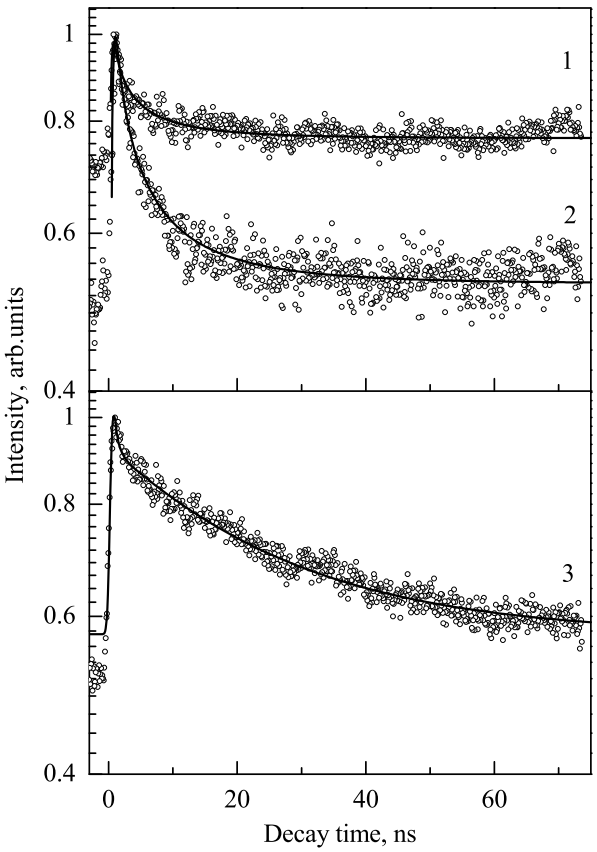

Figure 6: PL decay kinetics recorded for SrI_2:Nd crystal at T= 8 (1, 2) and 293 K (3) monitoring emission at E_m= 3.87 (1, 2) and 3.0 eV (3) upon excitation at E_{ex}= 5.29 (1) and 5.39 eV (2, 3).

3.4. Decay kinetics and time-resolved spectra

PL decay kinetics in nanosecond time-range. Fig. 6 shows the PL decay kinetics curves recorded for SrI_2:Nd crystals at T= 8 and 293 K monitoring emission at 3.0 and 3.87 eV upon excitation at E_{ex}= 5.29 and 5.39 eV. A significant portion of the light sum is due to the inertial components of the micro- and millisecond decay time-range shown in our measurements

Table 2: Parameters of the PL decay kinetics recorded for SrI_2:Nd crystals at temperature (T) monitoring emission at E_m upon excitation at E_{ex}: approximation parameter with the dimension of time (τ_0), average lifetime ($\bar{\tau}$), approximation parameter independent of time ($0 < \beta \leq 1$), amplitude (A) and pedestal (I_0) normalized to 100 conventional units at the observed maximum of the PL decay kinetics.

Parameter	E_m, eV		
	3.87	3.87	3.0[1]
β	0.5	0.5	1
T, K	8	8	293
E_{ex}, eV	5.29	5.39	5.39
I_0, arb.units	76.9	18.9	57.3
A, arb.units	52.9	40.9	15.0 / 17.6
τ_0, ns	1.6	1.8	0.5 / 25
$\bar{\tau}$, ns	9.6	10.8	0.5 / 25

[1)]kinetics was approximated by the sum of two exponential components.

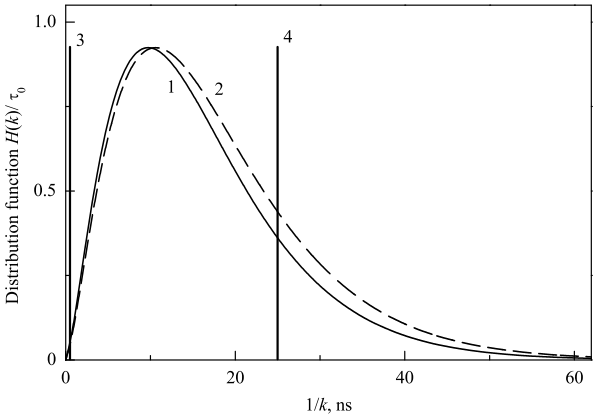

Figure 7: Distribution function $H(k)$ derived from the PL decay kinetics recorded for SrI_2:Nd crystal at T= 8 (1, 2) and 293 K (3, 4) monitoring emission at 3.87 (1, 2) and 3.0 eV (3, 4) upon excitation at E_{ex}= 5.29 (1) and 5.39 eV (2–4). The vertical lines symbolize the distribution functions in the form of $H(k) = \delta(k - 1/\tau_0)$.

in the form of a constant level – pedestal, Tab. 2. In all cases, the observed PL decay kinetics is not single-exponential, and it corresponds to the empirical relationship [26]

$$I(t) = I_0 + A \exp\left[-\left(\frac{t}{\tau_0}\right)^{\beta}\right], \quad (1)$$

where I_0 is a pedestal, taking into account the contribution of the inertial components; A is the amplitude of the exponential component; τ_0 is the approximation parameter that has the dimension of time; $0 < \beta \leq 1$ is a constant. Tab. 2 shows the results of the approximation.

The exponential term in equation (1) corresponds to the Kohlrausch relaxation function ('stretched exponent'), which is equivalent to a superposition of single-exponential components. Distribution of elementary relaxations through the reaction rate constants k is described by a continuous function $H(k)$ [26].

$$\frac{I(t) - I_0}{A} = \int_0^{\infty} H(k) \exp(-k\,t)\, \mathrm{d}k. \quad (2)$$

Fig. 7 showed the distribution functions $H(k)$, which have been calculated for the PL decay kinetics. These functions comprise two broad asymmetric peaks at 9.6 and 10.8 ns, corresponding to the curves recorded monitoring emission at the low-temperature PL band (E_m= 3.87 eV) upon excitation at E_{ex}= 5.29 and 5.39 eV, respectively. In the extreme case when β= 1, the Kohlrausch function becomes the ordinary exponent and peak in the distribution tends to the Dirac delta-function $H(k) = \delta(k - 1/\tau_0)$. This case is realized in our measurements at room temperature, where the PL decay kinetics is approximated by the sum of two exponential components with lifetimes τ_0= 0.5 and 25 ns, Fig. 6, 7 and Tab. 2.

Tab. 2 shows also the values of average decay time $\bar{\tau}$, calculated from formula [26]

$$\bar{\tau} = \tau_0 \frac{\Gamma(2/\beta)}{\Gamma(1/\beta)}, \quad (3)$$

where Γ is the Gamma function. For the exponent β= 0.5, the average decay time $\bar{\tau} = 6\,\tau_0$, which corresponds exactly to the position of the maximum in the $H(k)$ distribution, Fig. 7.

From a physical point of view, the observed distribution of the rate constants indicates a static distribution in the properties of the nearest environment of the luminescent center. This means that the processes occurring in one center will not affect the processes in other centers. The value β= 0.5 has been previously observed in the processes of diffusion-controlled quenching of the luminescence through the contact reactions [27, 28], and in processes of diffusionless resonance energy transfer through the dipole-dipole mechanism in various three-dimensional systems [29–31]. Two mechanisms of energy transfer to quenching centers were found for Nd^{3+} ions in YAG matrix [32]. At short decay times, a one-step energy transfer to randomly distributed quenching sites dominates, whereas energy migration to sinks consisting of cross-relaxing Nd ions dominates at long decay times. Under short-pulse excitation the luminescence decay is nonexponential for concentrations greater than about 1 at. % whereas at long-pulse excitation single exponential lifetimes

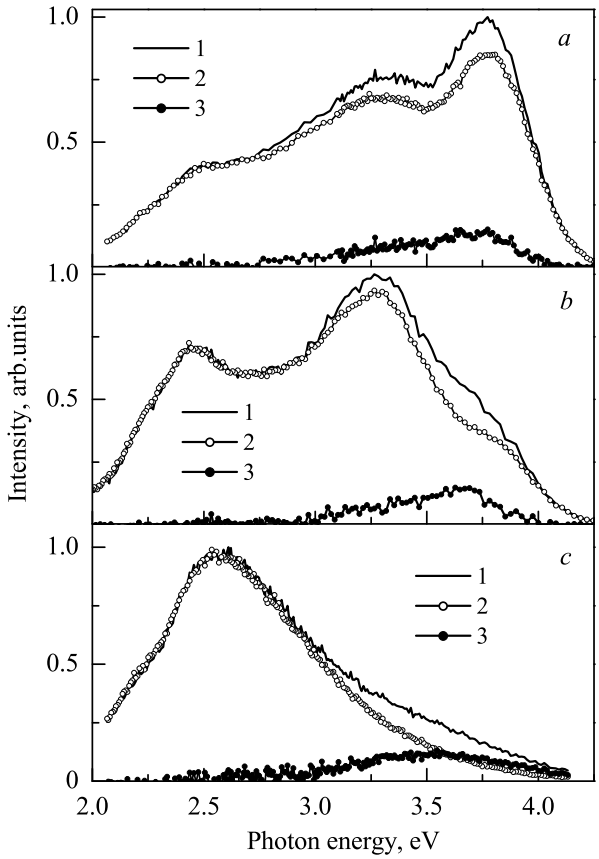

Figure 8: The time-resolved (TW) PL emission spectra recorded in the energy range of 2.0–4.5 eV for SrI_2:Nd crystal at 8 (*a*, *b*) and 293 K (*c*) monitoring emission at time-window TW1 (1) and TW2 (2) upon excitation at E_{ex}= 5.29 (*a*) and 5.39 eV (*b*). Curve (3) corresponds to the difference of normalized spectra TW1 and TW2.

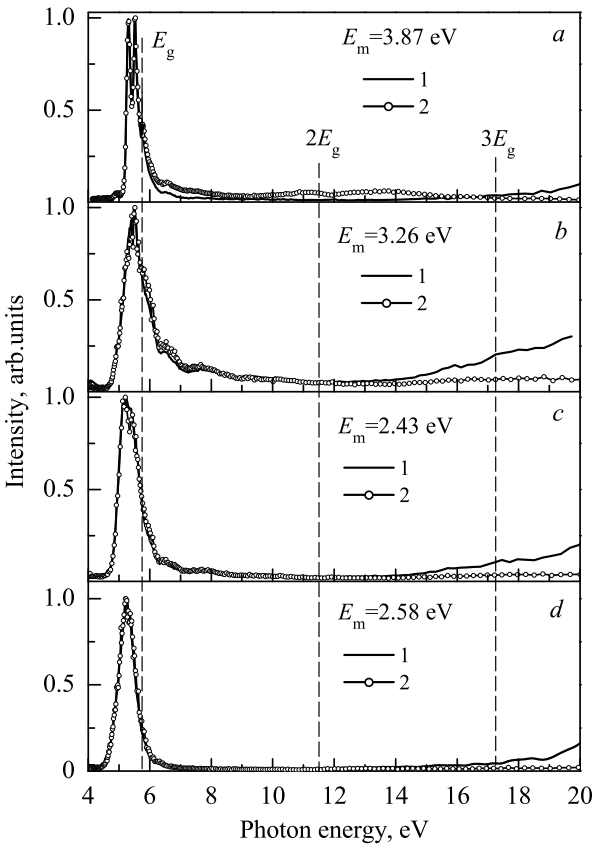

Figure 9: PLE spectra recorded for SrI_2:Nd crystal at 8 (*a*, *b*, *c*) and 293 K (*d*) monitoring emission at E_m in time-windows TW1 (1) and TW2 (2).

occurs even at Nd concentrations of a few percents [32]. The origin of the quenching centers can be attributed to the presence of large amount of hydroxyl groups [33], or the nanosecond kinetics of nonradiative relaxation of highly-quenched levels of Nd^{3+} ions [34]. The luminescence quenching can also occur due to quasidiffusion and stepwise migration in a disordered medium [35].

Time-resolved PL and PLE spectra. Fig. 8 shows the time-resolved photoluminescence spectra of SrI_2:Nd crystals recorded in the energy range of 2.0–4.5 eV. In the low-energy spectral region, where $g_1 \ldots g_3$ bands are located, the TW1 and TW2 spectra are identical in profile, so they are normalized to match the intensity in this spectral region. In the energy region where g_4 and g_5 bands are located, the time-resolved spectra TW1 and TW2 are different in profile. The difference of normalized spectra TW1 and TW2 gives an idea about the spectrum for the fast component of the PL decay kinetics. From Fig. 8 it follows that the spectrum of the fast component covers the g_4 and g_5 PL emission bands. This confirms indirectly our assumptions about the excitonic mechanism of energy transfer and the origin of the emission bands.

Fig. 9 shows PLE spectra recorded monitoring time-resolved emission at different PL bands. A common feature of all the spectra is the low PL intensity upon excitation in the energy range of interband transitions at $E_{ex} > E_g$. In combination with high photoluminescence intensity upon excitation at the fundamental absorption region $E_{ex} < E_g$ (exciton region), this indicates a high mobility and a high value of the diffusion length for electron excitations. At energies $E_{ex} > E_g$, the mean free path of photons in the crystal becomes comparable with the diffusion length of the electronic excitations, most of which can reach the surface and contribute to the surface energy losses due to non-radiative recombination. In addition, it indicates the insignificant role of the electron-hole recombination in the photolumines-

cence excitation in the SrI_2:Nd crystal.

In the energy range of $E_{ex} < 2.5\,E_g$, the TW1 and TW2 spectra are identical in profile. Some minor differences are observed only at E_m =3.87 eV (Fig. 9, *a*) in the TW2 spectrum. With further increase in the excitation energy, we observed a slow monotonic increase in the PL intensity of the TW1 spectrum, while the PL intensity in the TW2 spectrum remains virtually unchanged. The lifetime of the fast component of the PL decay kinetics which leads to the observed increase in the intensity, is much greater than the excitation pulse duration. Therefore, the observed increase in the luminescence intensity in the TW1 spectrum at $E_{ex} > 2.5\,E_g$ can not be attributed to instrumental reasons, such as increasing the contribution of the scattered light from the PL excitation channel. The most significant increase in the PL intensity in the TW1 spectrum occurs at E_m =3.26 eV (Fig. 9, *b*). This PLE spectrum relates mainly to the excitation of the PL emission band g_4, which is due to radiative annihilation of self-trapped excitons in SrI_2 crystal. Unfortunately, the excitation energy range in our study was only up to 20 eV, which is not enough to determine the reason of increase in the PLE intensity in the TW1 spectra. We have no reason to discuss in this paper the possibility of manifestation of the photon multiplication effect in SrI_2:Nd crystals. We can only note that in SrI_2:Eu crystals such effect was observed earlier in the PLE spectra recorded monitoring emission at 2.85 eV (Eu^{2+}), or 2.40 eV (crystalline hydrates) upon excitation in the energy range up to 40 eV [16]. The photon multiplication effect has been observed previously also in many alkali halides [36], binary oxides [37], nonlinear optical crystals [38–40]. Photon multiplication aspect in SrI_2:Nd crystals is a separate topic and could be origin of a special investigation. At this stage we can only say that SrI_2:Nd crystals exhibit mobile electronic excitations. Extremely low PLE intensity in the energy range from E_g to $3\,E_g$ (Fig. 9) is due to the high probability of migration for electronic excitations, which can easily reach the sinks of nonradiative relaxation.

4. Conclusions

We reported the results on the luminescence spectroscopy study of SrI_2:Nd crystals performed by the methods of luminescence VUV spectroscopy with a time resolution at 8 and 293 K. The main conclusions are as follows.

(1) Trivalent Nd^{3+} impurity can be introduced into the SrI_2 crystal lattice during the growth of these crystals by the vertical Bridgman method. The ratio of the ionic radii of Nd^{3+} and Sr^{2+} favors the heterovalent substitution of regular Sr^{2+} cation sites by the Nd^{3+} impurity ions. Compensation of the excess charge of the impurity ion in this case can be carried out by alkali metal ions or structural lattice defects. However, we can not exclude the possibility that the Nd^{3+} impurity ions can also occupy the interstitial voids.

(2) The results obtained by luminescence spectroscopy revealed the presence of trivalent Nd^{3+} impurity ions in the SrI_2 crystal lattice. At the same time, our results did not reveal the presence of divalent Nd^{2+} impurity ions in these crystals. The most intense luminescence band at ca.1070 nm is due to the radiative $^4F_{3/2} \rightarrow {}^4I_{11/2}$ transitions in Nd^{3+} ions. In the crystal transparency band, the most efficient excitation of the PL emission band occurs at either the optical transitions from the ground $^4I_{9/2}$ state to the lowest excited $^4F_{3/2}$ state or by charge transfer transitions $I^- \rightarrow Nd^{3+}$.

(3) Two elementary PL bands g_3 and g_5 with peaks at 2.8 and 3.8 eV we attribute to the presence of Nd^{3+} impurity ions in SrI_2 host lattice. The g_3 emission band is attributed to the luminescence of a lattice defect, possibly to the luminescence of the charge compensating defect, located in the vicinity of Nd^{3+} impurity ion. The g_5 band is presumably associated with radiative annihilation of self-trapped excitons in the defective areas of the SrI_2:Nd crystal.

(4) SrI_2:Nd crystals provide an efficient channel for exciton energy transfer from the matrix to the defect complexes discussed above. Two narrow intense peaks at 5.31 and 5.52 eV in the PLE spectrum of the intrinsic emission of SrI_2:Nd crystal are due to the creation of excitons in the vicinity of the defect complexes, and in a defect-free region of the crystal, respectively.

(5) The PL decay kinetics recorded for SrI_2 crystal monitoring emission at g_4 and g_5 bands upon excitation through the PLE excitonic bands, exhibits a nonexponential profile. Analysis of the PL decay kinetics using Kohlrausch function and restoring the distribution function $H(k)$ using the inverse Laplace transform, showed the presence of two broad asymmetric peaks at 9.6 and 10.8 ns in the distribution of the reaction rate constants, which indicate the presence of a static distribution on the properties of the nearest environment of the luminescent center.

All these observations do not encourage the development of Nd^{3+} doped strontium iodide as a scintillation crystal without additional doping by monovalent impurity ions.

Acknowledgments

This work was supported by the Siberian Branch of the Russian Academy of Sciences (Grant no.28) and partially supported by HASYLAB DESY (Project no.20110843).

References

[1] E.V.D. van Loef, P. Dorenbos, C.W.E. van Eijk, K. Krämer, and H.U. Güdel, Appl. Phys. Lett. 79 (10) (2001) 1573–575.
[2] K.S. Shah, J. Glodo, M. Klugerman, W.M. Higgins, T. Gupta, and P. Wong, IEEE Trans. Nucl. Sci. 51 (5) (2004) 2395–2399.
[3] N.J. Cherepy, S.A. Payne, S.J. Asztalos, G. Hull, J.D. Kuntz, T. Niedermayr, S. Pimputkar, J.J. Roberts, R.D. Sanner, T.M. Tillotson, E. van Loef, C.M. Wilson, K.S. Shah, U.N. Roy, R. Hawrami, A. Burger, L.A. Boatner, W.-S. Choong, and W.W. Moses, IEEE Trans. Nucl. Sci. 56 (3) (2010) 873–880.
[4] M.S. Alekhin, J.T.M. de Haas, K.W. Krämer, I.V. Khodyuk, L. de Vries, and P. Dorenbos, in: IEEE Nucl. Sci. Symp. Conf. Rec., Knoxville, TN, USA, 2010, pp.1589–1599.
[5] M.S. Alekhin, J.T.M. de Haas, K.W. Krämer, and P. Dorenbos, IEEE Trans. Nucl. Sci. 58 (5, Pt. 2) (2011) 2519–2527.
[6] C.M. Wilson, E.V. van Loef, J. Glodo, N. Cherepy, G. Hull, S. Payne, W.-S. Choong, W. Moses, and K.S. Shah, Proc. SPIE 7079 (2008) 707917(7).
[7] N.J. Cherepy, G. Hull, A.D. Drobshoff, S.A. Payne, E. van Loef, C.M. Wilson, K.S. Shah, U.N. Roy, A. Burger, L.A. Boatner, W.-S. Choong, and W.W. Moses, Appl. Phys. Lett. 92 (8) (2008) 083508.
[8] E.V. van Loef, C.M. Wilson, N.J. Cherepy, G. Hull, S.A. Payne, W.-S. Choong, W.W. Moses, K.S. Shah, IEEE Trans. Nucl. Sci. 56 (3) (2009) 869–872.
[9] D.H. Gahane, N.S. Kokode, P.L. Muthal, S.M. Dhopte, and S.V. Moharil, Opt. Mater. 32 (1) (2009) 18–21.
[10] J. Yu, L. Cui, H. He, Y. Hu, H. Wu, J. Zeng, and Y. Liu, Chem. Phys. Lett. 549 (2012) 32–38.
[11] X. Gao, Y.J. He, and Y.B. Chen, Optoelectron. Adv. Mater. Rapid Commun. 5 (4) (2011) 341–343.
[12] A.A. Kaminskii, V.S. Mironov, S.N. Bagaev, N.M. Khaidukov, M.F. Joubert, B. Jacquier, and G. Boulon, Phys. Status Solidi (a) 145 (1) (1994) 177–195.
[13] M. Karbowiak, P. Gnutek, and C. Rudowicz, Spectrochimica Acta Part A: Molecular and Biomolecular Spectroscopy 87 (2012) 46–60.
[14] G.H. Dieke, Spectra and Energy Levels of Rare Earth Ions in Crystals, (New York: Wiley Interscience, 1968).
[15] L.I. Isaenko and A.P. Yelisseyev, Chem. Sust. Develop. 8 (2000) 213–217.
[16] V.A. Pustovarov, I.N. Ogorodnikov, A.A. Goloshumova, L.I. Isaenko, A.P. Yelisseyev, Opt. Mater. 34 (5) (2012) 926–930.
[17] E.T. von Rietschel and H. von Bärnighausen, Z. Anorg. Allg. Chem. 368 (1969) 62–72.
[18] G. Zimmerer, Radiat. Meas. 42 (4–5) (2007) 859–864.
[19] A. Garcia, F. Guillen, and C. Fouassier, J. Luminesc. 33 (1) (1985) 15–27.
[20] A.M. Srivastava, S.J. Cammardello, H.A. Comanzo, and A. Meijerink, in: Meeting Abstracts – 218th Meeting of the Electrochemical Society, Vol. 1 of 3 of Meeting Abstracts 2010-02, Las Vegas, NV, 10–15th October 2010, Curran Associates, Inc., Red Hook, NY, 2011, abstr.no.2341.
[21] H. von Bärnighausen and E.T. Rietschel, Z. Anorg. Allg. Chem. 354 (1-2) (1967) 23–26.
[22] S.A. Hodorowicz and H.A. Eick, J. Solid State Chem. 46 (3) (1983) 313–320.
[23] R.D. Shannon, Acta Crystallogr. A32 (5) (1976) 751–767.
[24] J.W. Xu, J. Alloys Compd. 249 (1997) 213–216.
[25] D.S. McClure and Z.J. Kiss, J. Chem. Phys. 39 (12) (1963) 3251–3257.
[26] M.N. Berberan-Santos, E.N. Bodunov, and B.Valeur, Chem. Phys. 315 (2005) 171–182.
[27] E.W. Montroll, J. Chem. Phys. 14 (3) (1946) 202–211.
[28] S.A. Rice, Diffusion-limited reactions, Vol. 25 of Comprehensive Chemical Kinetics, (North Holland, Amsterdam: Elsevier, 1985).
[29] T. Förster, Z. Naturforsch. 4a (1949) 321–327.
[30] I.N. Ogorodnikov and V.A. Pustovarov, JETP Letters 96 (5) (2012) 308–312.
[31] I.N. Ogorodnikov and V.A. Pustovarov, J. Phys.: Condens. Matter. 24 (40) (2012) 405902(8).
[32] L.D. Merkle, M. Dubinskii, K.L. Schepler, and S.M. Hegde, Opt. Express 14 (9) (2006) 3893–3905.
[33] M. Pokhrel, N. Ray, G.A. Kumar, and D.K. Sardar, Opt. Mater. Express 2 (3) (2012) 235–249.
[34] T.T. Basiev and Yu.V. Orlovskii, Sov. Phys. JETP 69 (6) (1989) 1109–1118.
[35] M.V. Artamonova, C.M. Briskina, A.I. Burshtein, L.D. Zusman, and A.G. Skleznev, Sov. Phys. JETP 35 (3) (1972) 457–461.
[36] A. Lushchik, M. Kamada, M. Kirm, Ch. Lushchik, and I. Martinson, Radiat. Meas. 29 (3-4) (1998) 229–234.
[37] Ch. Lushchik, E. Feldbach, A. Frorip, M. Kirm, A. Lushchik, A. Maaros, and I. Martinson, J. Phys.: Condens. Matter. 6 (1994) 11177–11187.
[38] I.N. Ogorodnikov, V.A. Pustovarov, A.V. Kruzhalov, L.I. Isaenko, M. Kirm, and G. Zimmerer, Phys. Solid State 42 (3) (2000) 464–472.
[39] I.N. Ogorodnikov, V.A. Pustovarov, A.V. Kruzhalov, L.I. Isaenko, M. Kirm, and G. Zimmerer, Phys. Solid State 42 (10) (2000) 1846–1853.
[40] V.A. Pustovarov, I.N. Ogorodnikov, N.S. Bastrikova, A.A. Smirnov, L.I. Isaenko, A.P. Yelisseyev, Opt. Spectrosc. 101 (2) (2006) 234–244.